# A Novel Method for UHF RFID Tag Tracking Based on Acceleration Data

Andreas Parr, Robert Miesen, Fabian Kirsch, Martin Vossiek
Institute for Microwave Engineering and High Frequency Technology
University of Erlangen-Nuremberg
D-91058 Erlangen, Germany
andreas.parr@lhft.eei.uni-erlangen.de

*Abstract*— **Options for RFID tag tracking and localization are an essential asset for future high performance RFID reader systems. A reader with long reading range, high reading rate and multi-tag capability should be able to assist the user to find / retrieve tags, to create spatial object maps and to restrict the reading range to specific regions of interest. In this paper we introduce a novel method for RFID tag tracking with a moving – for example handheld – reader. An inertial measurement unit (IMU) is used to characterize the handheld trajectory. Contrary to approaches where IMU locations are reconstructed via double integration of the acceleration data, our novel technique only uses acceleration data without knowledge of the actual antenna locations. Inexpensive, standard inertial sensors can be used in this approach, and the usual drift and offset issues associated with IMU-based positioning are avoided. Parallel to the IMU acceleration data, the phase of the backscattered RFID signal is input. Double differentiation of the signal phase yields a second acceleration data set. By comparing the IMU and the RFID signal phase acceleration data, the direction of arrival of the RFID signal is estimated using a quasi-spatial optimal filter. This paper introduces the novel RFID tracking approach and illustrates its capability with numerical simulations and experimental results. This novel approach is a simple, yet promising, solution which can be implemented in any handheld reader and will improve its functionality considerably.**

***Keywords-UHF RFID; phase measurement; angle of arrival;***

## I. Introduction

While the extensive reading ranges of today's UHF RFID systems open up new opportunities, they also pose new challenges: like avoiding false positive readings and isolating and scanning the tag of interest in large tag populations. Thus RFID localization has become an area of intense interest [1]. Different approaches known from other wireless localization systems can also be applied to RFID systems. Received signal strength for example has been investigated extensively [2]. But RSS-based methods suffer severely from distortions in the propagation channel. Methods to mitigate these effects have been developed, e.g. the use of reference tags [3].

More recently, several methods based on phase evaluation have been proposed. Modern RFID readers provide the phase information of the backscatter signal, which can be used to detect relative movements and for direction of arrival estimation [4]. Absolute tag distances can be measured by utilizing more than one carrier frequency [5]. The overall bandwidth of multi-frequency approaches is restricted by regulations. This makes precise and reliable ranging a challenging task, especially in multipath environments [6]. Multiple angles of arrival (AoA) can be obtained from phase measurements with antenna arrays. Subsequently the tag location can be retrieved by multi-angulation [7]. Coherent superposition of phase values measured with a single antenna at multiple locations and at different times, forming a synthetic aperture is another option [8]. Utilizing synthetic apertures for RFID localization is a promising approach since the resulting resolution is significantly higher compared to ordinary antenna arrays. Localization systems based on synthetic apertures are known from [9] and [10]. Absolute or relative positioning, or combinations of both, can be used to determine the antenna trajectory [11]. A combination of those two methods is beneficial in order to achieve short, as well as long-term, accuracy of the determined locations [12].

Determining the locations of a freely moving antenna is nonetheless a challenging task. In phase-based remote sensing technologies, antenna position errors have to be significantly below the wavelength of the carrier signal to ensure the recorded data is coherently processed.

In [9-12] inertial measurement units are proposed to retrieve positional information. An inertial measurement unit measures accelerations and rotations in 3D space. It provides high quality short-term positional information but accumulates errors due to the integration of the sensor data. For this reason low-cost IMUs with high random errors can be a critical factor in a system using a synthetic aperture.

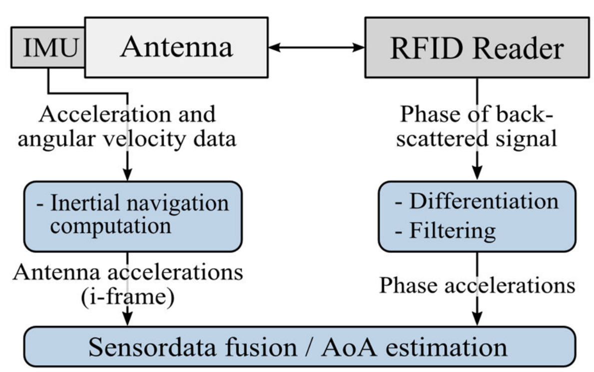


Figure 1. Block diagram of sensors and associated signal processing of the proposed direction finding method.

In this paper we propose a new phase-based method which utilizes a synthetic aperture – characterized only by the accelerations of a single moving antenna without calculating the antenna locations – thus avoiding errors introduced by integrating antenna acceleration data. The phase acceleration between interrogator and transponder is determined by double differentiation of the measured phase values. It is subsequently evaluated with respect to the physical antenna accelerations, see Fig. 1.

The theoretical approach and associated simulation results are presented first, followed by error discussions and the measurements conducted.

## II. Array Definition, Inertial Navigation And Geometric Relations

A synthetic antenna aperture is typically formed out of a single antenna element which gathers signals at different positions $\vec{r}_{a,i}$ at times $t_i$ with $i \in 1,2,...,n$ in a time interval $T$.

The higher order differentiates of the antenna positions, such as the antenna velocities $\vec{v}_{a,i}$ and the antenna accelerations $\vec{a}_{a,i}$ contain additional information about the properties of the synthetic aperture. The accelerations are of particular interest in the technique proposed in this paper.

The antenna accelerations $\vec{a}_{a,i}$ in a time invariant inertial coordinate system (i-frame) can be derived from the antenna accelerations $\vec{a}^b_{a,i}$ and the angular velocities $\vec{\omega}^b_i$, measured by an IMU in the body fixed coordinate system (b-frame) [13]. For an IMU update rate that is high compared to the rate of change of $\vec{\omega}^b_i$, the change of attitude $\Delta\vec{\sigma}_i$ between both coordinate systems in a single time interval can be approximated by

$$\Delta\vec{\sigma}_i \approx \vec{\omega}^b_i \cdot (t_i - t_{i-1}). \tag{1}$$

A quaternion $\Delta q_i$ is used to represent the corresponding rotation during the time interval:

$$\Delta q_i = \begin{pmatrix} \cos\dfrac{\Delta\sigma_i}{2} \\ \dfrac{\Delta\vec{\sigma}_i}{\Delta\sigma_i}\sin\dfrac{\Delta\sigma_i}{2} \end{pmatrix} \quad , \quad \Delta\sigma_i = \left|\Delta\vec{\sigma}_i\right|. \tag{2}$$

The momentary quaternion $q_i$ describing the rotation between i- and b-frame is given by

$$q_i = q_{i-1}\,\Delta q_i. \tag{3}$$

It is used to transform the measured accelerations into the i-frame [14]. The initial relationship $q_0$ between both coordinate systems can be set to the quaternion $(1\ 0\ 0\ 0)^T$ representing no rotation. Hence, the i-frame matches the b-frame at the beginning of the measurement. However, we still need to measure the gravity vector in the i-frame initially in order to subtract it correctly from the measured acceleration at all timestamps, to obtain only the accelerations that are caused by antenna movement.

With an initial gravity measurement and by evaluating the geomagnetic field strength, $q_0$ can be determined in a way that the resulting i-frame matches the earth fixed coordinate system (e-frame). This is necessary if the tag directions shall be obtained in the e-frame. In order to obtain the antenna accelerations in the i-frame, the accelerations measured in the b-frame are rotated and corrected by the external measurement offsets $\Delta\vec{a}_{a,i}$, to yield:

$$\begin{pmatrix} 0 \\ \vec{a}_{a,i} \end{pmatrix} = \left(0\ a_{a,x,i}\ a_{a,y,i}\ a_{a,z,i}\right)^T = q_i \begin{pmatrix} 0 \\ \vec{a}^b_{a,i} \end{pmatrix} q_i^{-1} - \begin{pmatrix} 0 \\ \Delta\vec{a}_{a,i} \end{pmatrix}. \tag{4}$$

Fig. 2 shows the system geometry of a synthetic aperture with associated values and notations. The geometric center of the synthetic aperture is given by the centroid of all sampling antenna positions:

$$\vec{C}_a = \frac{1}{n}\sum_{i=0}^{n} \vec{r}_{a,i}\,. \tag{5}$$

## III. Phase Processing

The carrier phase $\varphi_i$ associated with the distance $\left|\vec{d}_{at,i}\right|$ between reader antenna and RFID tag and the carrier wavelength $\lambda_c$ expressed by

$$\varphi_i = \frac{2\pi}{\lambda_c} 2 d_{at,i} \bmod 2\pi\,, \quad d_{at,i} = \left|\vec{d}_{at,i}\right|, \tag{6}$$

can be measured with the moving antenna attached to a standard RFID reader simultaneously to the antenna accelerations.

The phase acceleration between antenna and tag is retrieved by taking the second derivative of the unwrapped phase values $\varphi_i$. We use a digital derivative filter that has been adapted to the aperture geometry, to the velocity of the antenna movement, and to the signal-to-noise ratio of the collected phase samples.

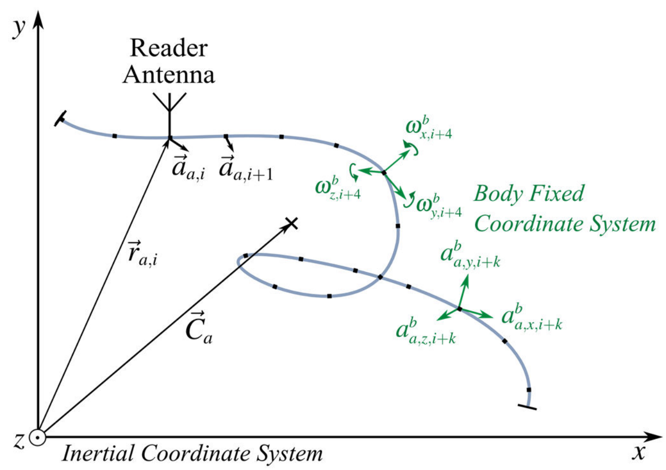


Figure 2. Geometry of the synthetic aperture formed by a moving antenna described by positions, accelerations and rotations in the inertial coordinate system and the body fixed coordinate system.

To apply identical scaling and proportionality to the acceleration data scanned by the inertial sensors, the measured phase acceleration is expressed in m/s$^2$ and denoted by $a_{\varphi,i}$: thus, according to (6):

$$a_{\varphi,i} = \frac{\lambda_c}{4\pi} \frac{\Delta^2 \varphi_i}{\Delta t^2}. \quad (7)$$

It should be noted, that the value margin that is limited to $[0, 2\pi]$ when evaluating phase values, is expanded to an unlimited value margin for the phase accelerations. This has advantages for the array signal processing since the ambiguous angles resulting from a single phase acceleration value are significantly reduced.

## IV. Direction Finding Method

The proposed method is designed to determine the direction of the vector $\vec{d}_{at}^{C} = \vec{r}_t - \vec{C}_a$ pointing from $\vec{C}_a$ towards the coordinates of the transponder at $\vec{r}_t$. The measured phase accelerations $a_{\varphi,i}$ ideally match the projection of the negative antenna accelerations onto the vector $\vec{d}_{at,i}$:

$$a_{\varphi,i} = -\frac{\vec{a}_{a,i}^{T} \cdot \vec{d}_{at,i}}{d_{at,i}}. \quad (8)$$

For a large distance between tag and antenna compared to the biggest span $L$ of the synthetic aperture perpendicular to $\vec{d}_{at}^{C}$ (Fig. 3), $\vec{d}_{at,i} / d_{at,i}$ can be approximated by $\vec{d}_{at}^{C} / d_{at}^{C}$ with $d_{at}^{C} = \left|\vec{d}_{at}^{C}\right|$:

$$a_{\varphi,i} = -\frac{\vec{a}_{a,i}^{T} \cdot \vec{d}_{at}^{C}}{d_{at}^{C}} \text{ for } d_{at,i} \gg L \quad (9)$$

This approximation is an essential feature of the proposed method since no antenna positions are calculated or used in the AoA derivation. The AoA calculation just assumes that the antenna is defined in a single position at $\vec{d}_{at}^{C}$ with $n$ different antenna accelerations.

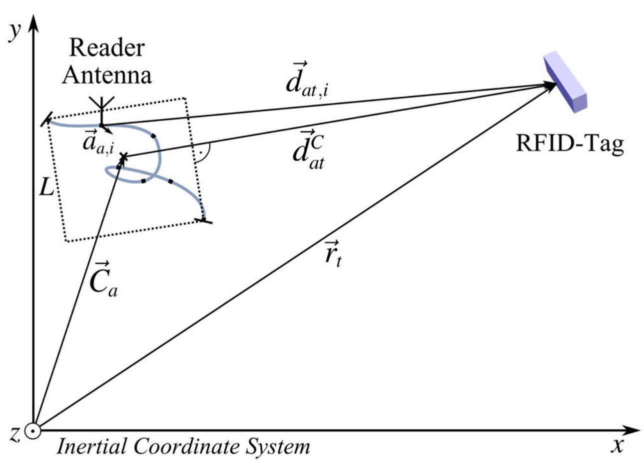


Figure 3. Basic geometry of a measurement situation in which an RFID tag is interrogated from the moving reader antenna.

Based on (9), the proposed method forms direction-dependent hypotheses for the phase accelerations. Therefore the negative measured antenna acceleration vectors $-\vec{a}_{a,i}$ are rotated around the axes of the inertial coordinate system and projected onto a unity vector $\vec{w}$. The hypotheses for all possible rotations are given by

$$a_{\varphi,\text{hypo},i}(\gamma_x, \gamma_y, \gamma_z) = -\vec{w} \cdot (\mathbf{R}_z(\gamma_z)\mathbf{R}_y(\gamma_y)\mathbf{R}_x(\gamma_x)\,\vec{a}_{a,i}), \quad (10)$$

with $\mathbf{R}_{x,y,z}$ being the rotation matrices for rotations around the three i-frame axes by the angles $\gamma_{x,y,z}$. We choose $\vec{w} = (1\ 0\ 0)$ and reduce the rotations by setting $\gamma_x = 0$, $\gamma_y \in [0, 2\pi]$ and $\gamma_z \in [-\pi, \pi]$. The angles $\gamma_y$ and $\gamma_z$ now represent Azimuth and Elevation in the i-frame and are sufficient to rotate all $\vec{a}_{a,i}$ in any direction.

Substituting $\vec{w}$ and $\mathbf{R}_{x,y,z}$, (10) can be simplified to:

$$\begin{aligned} a_{\varphi,\text{hypo},i}(\gamma_y, \gamma_z) = & -\cos(\gamma_y)\cos(\gamma_z)\ a_{a,x,i} \\ & + \sin(\gamma_z)\ a_{a,y,i} \\ & - \sin(\gamma_y)\cos(\gamma_z)\ a_{a,z,i}. \end{aligned} \quad (11)$$

The least squares method, which corresponds to a spatial optimal filter for a Gaussian error model, is used to test the hypotheses. The squared differences between $a_{\varphi,i}$ and $a_{\varphi,\text{hypo},i}(\gamma_y, \gamma_z)$ are summed over all $n$ timestamps for all possible rotation angles. The target function $I$ which has to be minimized with respect to $\gamma_y$ and $\gamma_z$ is given by

$$I(\gamma_y, \gamma_z) = \sum_{i=1}^{n} \left[ a_{\varphi,i} - a_{\varphi,\text{hypo},i}(\gamma_y, \gamma_z) \right]^2. \quad (12)$$

The vector $\vec{w}$ rotated in the opposite direction by the angles leading to the minimum of the target function $I_{\min} = I(\gamma_y', \gamma_z')$, is the estimate for the unity direction vector pointing towards the transponder:

$$\frac{\vec{d}_{at,\text{est}}^{C}}{d_{at,\text{est}}^{C}} = \mathbf{R}_y(-\gamma_y')\mathbf{R}_z(-\gamma_z')\,\vec{w} = \begin{pmatrix} \cos(\gamma_y')\cos(\gamma_z') \\ \sin(-\gamma_z') \\ \sin(\gamma_y')\cos(\gamma_z') \end{pmatrix}. \quad (13)$$

In other words, the algorithm searches for an AoA vector in 3D space that, if the antenna accelerations are projected onto it, leads to a new vector, whose length best matches the negative tag accelerations relative to the antenna for all time stamps.

Fig. 4 shows an example of a target function which was evaluated for a single data point (n = 1). The antenna acceleration $\vec{a}_{a,1}$ and the transponder at $\vec{d}_{at,1}$ lead to a cone shaped minimum of the target function due to the rotational symmetry of the single antenna acceleration vector. One can imagine how the resulting cones for multiple data points can lead to an unambiguous minimum at the transponder direction if the directions of $\vec{a}_{a,i}$ differ for at least three timestamps. Thus antenna acceleration vectors which point in the same direction generate redundant information that will not improve the

tracking capabilities of the synthetic acceleration aperture. This effect is similar to using the same positions at multiple timestamps when forming a normal position based synthetic aperture.

In this paper we use a grid search to find the angles of rotation leading to $I_{\min}$. Errors arise from the search grid density over $\gamma_y$ and $\gamma_z$ which lead to a lower boundary for the RMS angle error, via:

$$\overline{f}_{g,\mathrm{RMS}} = \sqrt{\left(\frac{\Delta\gamma_y}{\sqrt{12}}\right)^2 + \left(\frac{\Delta\gamma_z}{\sqrt{12}}\right)^2}, \tag{14}$$

with $\Delta\gamma_{y,z}$ being the angles between adjacent grid points. More advanced algorithms with lower computational costs compared to the achievable accuracy can be applied to determine the target function minimum.

## V. Simulations and Error Discussions

We carried out simulations to estimate the accuracy of the algorithm for possible application scenarios. We assume that the antenna is attached to a device which is moved in all spatial directions following a sinusoidal pattern with: an equal span $L'$ in all Cartesian directions, the swaying frequencies $f_{s,xyz}$ and random starting phases $\tilde{\varphi}_{s,xyz}$ between 0 and $2\pi$:

$$\vec{r}_a(t) = \frac{L'}{2}\begin{pmatrix} \sin(2\pi f_{s,x} t + \tilde{\varphi}_{s,x}) \\ \sin(2\pi f_{s,y} t + \tilde{\varphi}_{s,y}) \\ \sin(2\pi f_{s,z} t + \tilde{\varphi}_{s,z}) \end{pmatrix}. \tag{15}$$

Measurement errors for the resulting phase accelerations and the antenna accelerations are represented by

$$\vec{a}'_{a,i} = \vec{a}_{a,i} + \begin{pmatrix} \tilde{a}_{a,x,i} \\ \tilde{a}_{a,y,i} \\ \tilde{a}_{a,z,i} \end{pmatrix} + a_{\mathrm{drift}} \frac{t_i}{\mathrm{s}} \begin{pmatrix} 1 \\ 1 \\ 1 \end{pmatrix}, \tag{16}$$

$$a'_{\varphi,i} = a_{\varphi,i} + \tilde{a}_{\varphi,i}, \tag{17}$$

with

$\tilde{a}_{a,xyz,i} \sim \mathcal{N}(\mu = 0, \sigma = R \cdot \overline{a}_{xyz})$ and $\tilde{a}_{\varphi,i} \sim \mathcal{N}(\mu = 0, \sigma = R \cdot \overline{a}_{\varphi})$,

where $\tilde{a}_i$ are random numbers taken from a zero-mean normal distribution $\mathcal{N}$, $\overline{a}_{xyz}$ and $\overline{a}_{\varphi}$ are the mean acceleration values of the trajectories used and $R$ is a scalar acceleration error factor. A linear drift over time of the antenna acceleration data, representing the acceleration error due to a false gravity correction, is represented by $a_{\mathrm{drift}}$. Measurements with the used IMU for no movement showed that the rotational drift $\omega_{\mathrm{drift}}$ is about 0.05 °/s which causes an $a_{\mathrm{drift}}$ of $0.01\,\mathrm{m/s^3}$ for small movement durations. Nevertheless the actual error model is more complex depending on the application, the sensor technology and the measurement time.

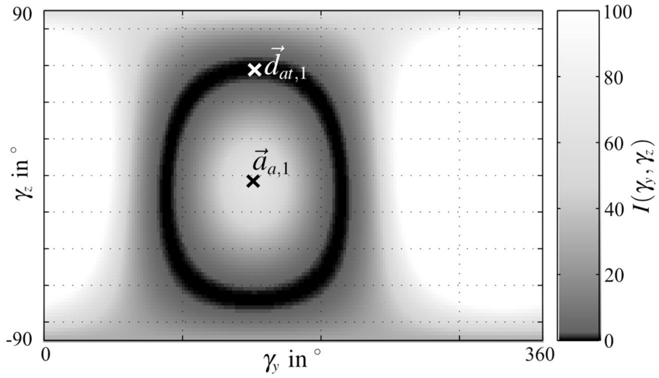


Figure 4. Target Function $I$ for a transponder at the direction $\vec{d}_{at,1}$ and a single acceleration data point $\vec{a}_{a,1}$. As visible a single measurement cannot reveal the actual tag direction, since $I$ reaches its minimum value along a cone shaped ambiguity due to the rotational symmetry of the acceleration vector.

The simulated RMS direction error $\Delta\delta_{RMS}$ with

$$\Delta\delta = \arccos\left(\frac{\vec{d}^{\,C}_{at} \cdot \vec{d}^{\,C}_{at,\mathrm{est}}}{d^{C}_{at} \cdot d^{C}_{at,\mathrm{est}}}\right), \tag{18}$$

is used for evaluating the simulation results. For each mean error, 2 000 iterations with random motions and random tag directions were evaluated for $\Delta\gamma_y = \Delta\gamma_z = 2°$ leading to $\overline{f}_{g,RMS} = 0.82°$. The IMU and tag phase update rate is set to $R_r = 50\,\mathrm{Hz}$ and the swaying frequencies are equally distributed as $1\,\mathrm{Hz} < f_{s,xyz} < 2\,\mathrm{Hz}$ and different in all three dimensions. The trajectory span was set to $L' = 0.3\,\mathrm{m}$ producing mean acceleration values $\overline{a}_{xyz} = 16\,\mathrm{m/s^2}$ and $\overline{a}_{\varphi} = 8\,\mathrm{m/s^2}$.

Fig. 5 shows the error $\Delta\delta_{RMS}$ versus the acceleration noise factor $R$ evaluated for different movement times $T$. The following parameters were also set: $d^{C}_{at} = 3\,\mathrm{m}$ and $a_{\mathrm{drift}} = 0$.

For low noise the RMS error is dominated by the grid error but still similar for the different measurement times. At higher random errors, increased measurement time produces comparatively smaller AoA errors since more data sets are evaluated, which leads to enhanced noise suppression and to an aperture with lower symmetry and correlation between the acceleration data points, which, is advantageous for reducing

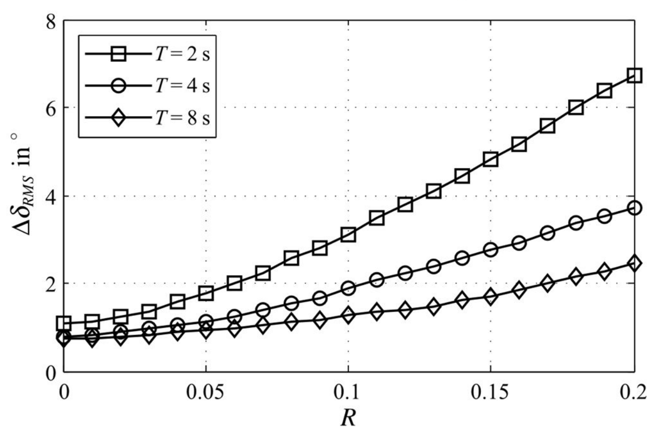


Figure 5. Simulated direction error $\Delta\delta_{RMS}$ versus acceleration error $R$ for different motion time durations $T$ and $a_{\mathrm{drift}} = 0$.

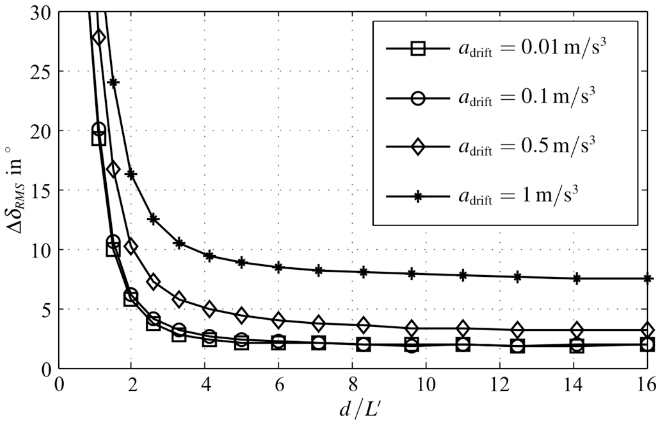


Figure 6. Simulated direction error $\Delta\delta_{RMS}$ versus antenna tag distance for different antenna acceleration drifts $a_{drift}$ .

ambiguities known from array processing. The simulation results show that the proposed method is capable of determining the AoA with an accuracy of less than 4° for the above scenario if the acceleration errors are kept at moderate levels (R < 10 %).

Fig. 6 shows the RMS error versus the antenna to tag distance described by the relation $d/L'$ according to (9) for different antenna acceleration drifts, $R = 0.1$ and $T = 4\,s$. All other parameters were kept as before. It can be seen that the approximation made in (9) fails for small antenna to tag distances. However for typical reading distances greater than 1m the error remains below 5° for the described trajectory if drift errors are kept at normal levels.

The simulations show that, as neither antenna velocity nor location have to be derived via integration, quite a high degree of robustness against accelerometer noise and drift is achieved.

In real world applications however the phase error which causes a phase acceleration error also depends on multipath. Reflection and refraction lead to different travel distances for the backscattered signal and hence to a phase that deviates from the free space propagation model.

A method for mitigating multipath effects using Doppler shifts is proposed in [15] for synthetic aperture applications. This approach could also prove useful for improving the method proposed in this paper. Using multiple carrier frequencies can also help suppress multipath effects. However, the reduced reading rate per frequency reduces the number of phase values available for reconstructing the phase acceleration. This is especially a problem if no proper phase unwrap can be applied to the phase values prior to differentiation.

Additionally an angle-dependent antenna phase characteristic can introduce errors as well and should therefore be taken into account during antenna design. Also, only a certain zone can be scanned with a handheld antenna in most applications due to the angle-dependent antenna gain.

## VI. MEASUREMENTS

The proposed method was evaluated with measurements using a self-designed low-cost inertial measurement unit with three gyroscopes and three accelerometers. The IMU was attached to the reader antenna with 8.5 dBi gain. The EPC Gen2 compliant RFID reader emits a signal at 866 MHz with a signal strength of 2 W ERP.

Four RFID tags were placed at a distance of 3 m to the antenna. Two different test setups were evaluated, one in an anechoic chamber (Fig. 7) and the other in a room with several metal structures to foster strong multipath propagation (Fig. 8).

The antenna was swayed several times for about 8-12 s providing about 500 datasets for each tag. We tried to perform similar movements to the ones used in the simulations stated under (15) with no intended rotations. The example in Fig. 9 shows part of a single performed trajectory which produced the processed phase and antenna accelerations data displayed in Fig. 10. Fig. 11 shows the actual directions of the four RFID tags and the estimates of the direction vectors for several measurements.

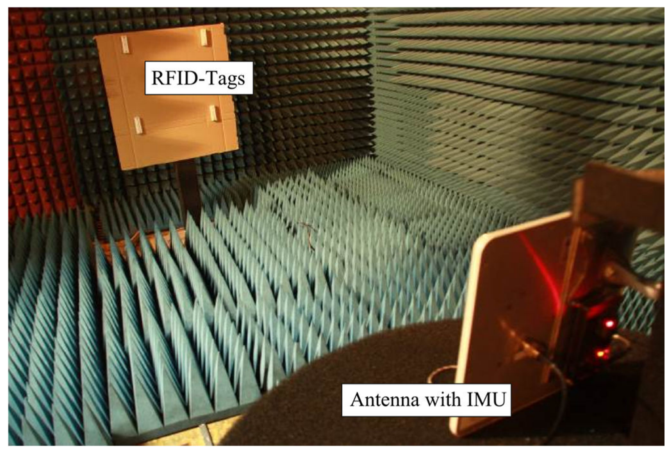


Figure 7. Test setup with four RFID tags, antenna and IMU placed in an anechoic chamber.

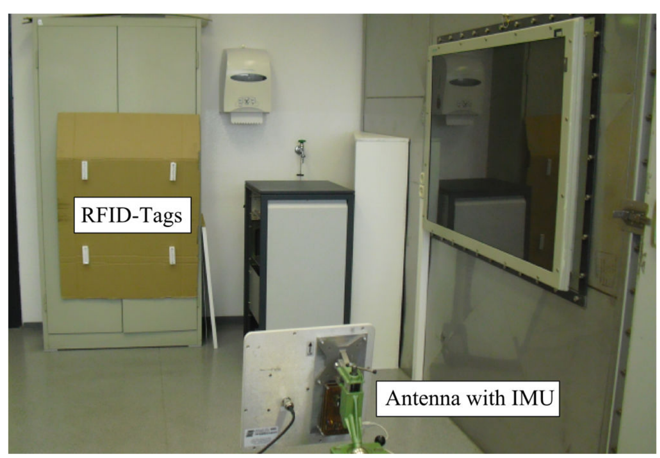


Figure 8. Test setup in multipath influenced environment with a metal wall on the right and a metal shelf behind the tags.

The RMS angle error according to (18) was 1.9° for the anechoic chamber test setup. In the second test setup including multipath, the RMS error increased to 5.1°. The unknown orientation between the IMU (b-frame) and the test environment (e-frame) described by the initial rotation quaternion $q_0$ was determined with an initial gravity measurement and by removing the remaining mean azimuth offset over the four tags for each measurement. Thus part of the bias error caused by systematic effects was removed as well.

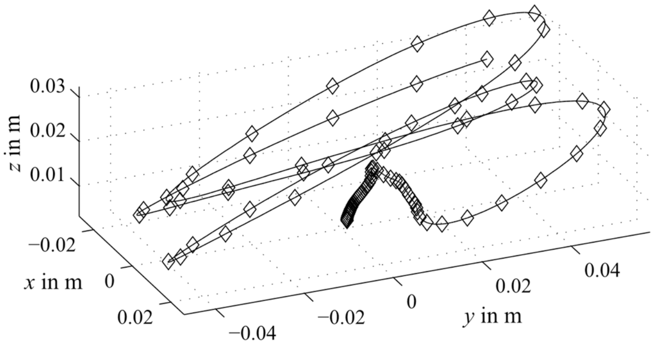

Figure 9. Example of test trajectory $\vec{r}_{a,i}$ estimated from input IMU-Data.

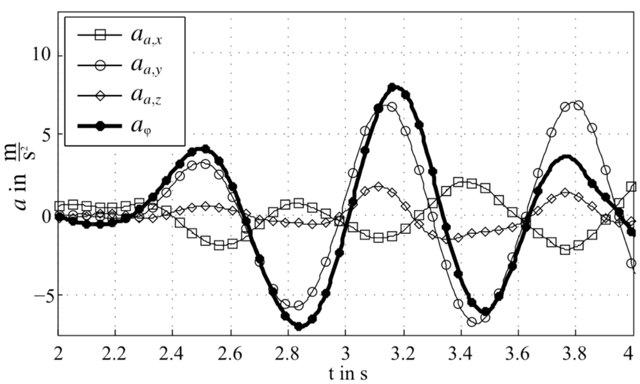

Figure 10. Antenna and phase accelerations extracted from the measurements.

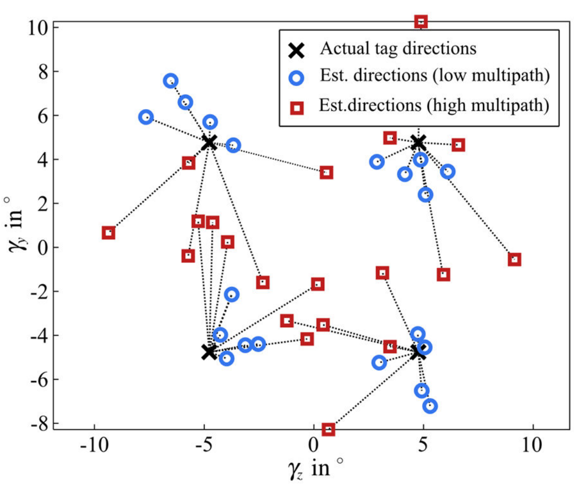

Figure 11. Comparison of direction estimates and actual tag positions for low and high multipath measurements.

A handheld reader used to guide an operator to a tag of interest can avoid the task of determining this relationship by using augmented reality technology. A handheld device equipped with a camera and a display could visualize the directions found in the pictures that were taken during the movement and present the result to the user [16].

## VII. Conclusion

A novel method for estimating the angle of arrival of standard UHF RFID tags has been presented. This method enhances handheld readers so they can guide the user to specific tags. As shown a short period of accelerated reader antenna movement is sufficient to retrieve an angle of arrival with an uncertainty well below 10° under multipath conditions. We are currently designing a revised IMU as well as an embedded online data processing system for improved synchronization between IMU and reader data. Another planned enhancement is the visual indication of the tag direction using an augmented reality approach.

## References


[1] R. Miesen *et al.*, "Where is the Tag?," *IEEE Microwave Magazine*, vol.12, no.7, pp. 49-63, Dec. 2011.

[2] J. Hightower, G. Borriello and R. Want, "SpotON: An Indoor 3D Location Sensing Technology Based on RF Signal Strength," Univ. of Washington, Washington, DC, CSE Tech. Rep. #2000-02-02, Feb. 2000.

[3] L. M. Ni *et al.*, "LANDMARC: indoor location sensing using active RFID," in *Proc. Pervasive Computing and Communications,* 2003, pp. 407-415.

[4] P. V. Nikitin *et al.*, "Phase based spatial identification of UHF RFID tags," in *Proc. IEEE International Conference on RFID*, 2010, pp. 102-109.

[5] X. Li, Y. Zhang, and M. G. Amin, "Multifrequency-based range estimation of RFID Tags," in *Proc. IEEE International Conference on RFID,* 2009, pp. 147-154.

[6] G. Li *et al.*, "Bandwidth Dependence of CW Ranging to UHF RFID Tags in Severe Multipath Environments," in *Proc. IEEE International Conference on RFID,* 2011, pp. 19-25.

[7] S. Azzouzi *et al.*, "New measurement results for the localization of UHF RFID transponders using an Angle of Arrival (AoA) approach," in *Proc. IEEE International Conference on RFID,* 2011, pp. 91-97.

[8] R. Miesen, F. Kirsch, and M. Vossiek, "Holographic localization of passive UHF RFID transponders," in *Proc. IEEE International Conference on RFID,* 2011, pp. 32-37.

[9] P. Gulden *et al.,* "Radiobased locating system provided with a synthetic aperture," U.S. Patent 7 948 431 B2, May 24, 2011.

[10] Nielsen *et al.,* "Handheld synthetic antenna array." U.S. Patent 2011/0070840 A1, Mar. 24, 2011.

[11] H. Wu, T. Zwick, "Automotive SAR for parking lot detection," in *Proc. German Microwave Conference,* 2009, pp. 1-8.

[12] T.A. Kennedy, "Strapdown inertial measurement units for motion compensation for synthetic aperture radars," in *IEEE Aerospace and Electronic Systems Magazine*, vol.3, no.10, pp.32-35, Oct. 1988.

[13] Aerospace & Electronic Systems Society, "IEEE Standard for Inertial Systems Terminology," IEEE Std 1559-2009, Jan. 2005.

[14] Y. Wu *et al.*, "Strapdown inertial navigation system algorithms based on dual quaternions," in *IEEE Trans. Aerosp. Electron. Syst.*, vol.31, no.1, Jan. 2005.

[15] S. Draganov *et al.*, "Synthetic aperture navigation in multipath environments," in *IEEE Wireless Communications*, vol.18, no.2, pp. 52-58, Apr. 2011.

[16] S. Kunkel *et al.*, "SAR-like localization of RFID tags for non-uniform trajectory," *European Wireless Technology Conference*, 2010, pp.281-284.